

Multi-Wavelength Analytical Ultracentrifugation of Human Serum Albumin complexed with Porphyrin

Courtney N. Johnson | UTHSCSA, Dept. of Biochemistry and Structural Biology, San Antonio, Texas

Heidi Ramsower | UTSA, Dept. of Physics and Astronomy, San Antonio, Texas

Julio Urquidi | UTSA, Dept. of Physics and Astronomy, San Antonio, Texas

Lorenzo Brancaleon | UTSA, Dept. of Physics and Astronomy, San Antonio, Texas

Borries Demeler | UTHSCSA, Dept. of Biochemistry and Structural Biology, San Antonio, Texas

Abstract

Analytical Ultracentrifugation (AUC) is the method of choice to characterize colloidal systems under physiological solution conditions. Recently, a novel multi-wavelength (MWL) detector on Beckman Coulter's Optima AUC has been developed, which for the first time, couples the hydrodynamic separation of colloidal mixtures to spectral deconvolution of interacting and non-interacting solutes present in a mixture. We show here how one can take advantage of the in Sorét band of porphyrins complexed with different cations to spectrally deconvolute dissimilar optical properties from different molecules. Several sites in Human Serum Albumin (HSA) have been postulated to possess the ability to directly bind metal ions as well as organometallic compounds. The evidence has generated a lot of interest in the physiological role of HSA as a metal binding protein but also as a vehicle for synthetic biology uses of the metal binding properties (e.g., synthetic blood and solar energy conversion). One of the most intriguing and potentially useful among these interaction is the ability of HSA to bind heme and other metallo-porphyrins. We show here how MWL-AUC on the Optima AUC can baseline-separate even minute changes in hydrodynamic shape and size between HSA-PPIX and apo-HSA.

Methods

Binding and Purification of HSA-PPIX

Human Serum Albumin (HSA), dimethylsulfoxide (DMSO) were purchased from Sigma-Aldrich (St. Louis, MO). Tin-Chloride (Sn(IV) PPIX) was purchased from Frontier Scientific Inc. (Logan, UT). Solid Sn(IV)PPIX was dissolved in DMSO. This was then diluted out to create an aqueous stock containing <1% DMSO. HSA was added to this aqueous stock then dialyzed and subsequently centrifuged to create an aggregate free solution.¹

UV Spectroscopy

The UV/visible spectra of apo-HSA and HSA complexed with porphyrin were measured on a benchtop spectrophotometer. A maximum absorption of the porphyrins is found at the Sorét band between 370-420 nm. The maximum absorption of the HSA is ~278 nm (see Figure 1).¹ The actual values were used to determine the concentration of HSA and monomerized porphyrins in each sample.

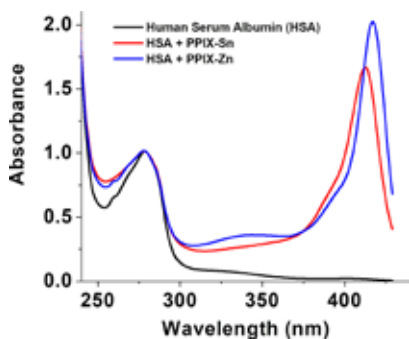


Figure 1. Absorbance spectra of Human Serum (HSA), HSA+PPIX-Sn and HSA+PPIX-Zn

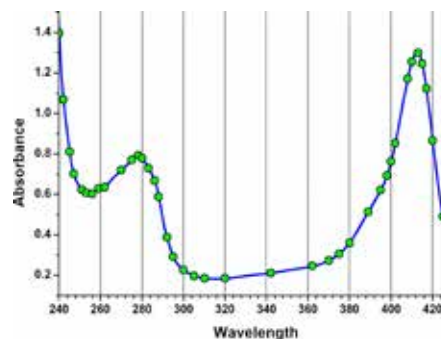


Figure 2. Plot of measured wavelengths (green circles). Wavelengths were chosen to emphasize regions of the spectrum where the absorbance has the greatest degree of change.

Analytical Ultracentrifugation

Sedimentation velocity experiments were performed at 45000 rpm and 20°C. Samples were placed into cells fitted with epon centerpieces and quartz windows. Additional samples were measured in 10 mM NaPO4 buffer. The experiments were performed with the new Beckman Optima AUC multi-wavelength instrument equipped with both absorbance and Rayleigh interference optics. 42 wavelengths were measured in intensity mode. Wavelengths were positioned to assure that linear interpolations of the spectrum would generate the smallest RMSD difference between the interpolation and the measured spectrum. This approach emphasizes regions of the spectrum where the absorbance rapidly changes. 45 scans were collected for each wavelength over a 10.5 hour period.

AUC-MWL Data Analysis

All data were analyzed with UltraScan-III version 2352.² Sedimentation velocity data were edited by defining meniscus, data range and plateau for each wavelength. The meniscus was fitted with the 2-dimensional spectrum analysis (2DSA)³, with simultaneous subtraction of time- and radially invariant noise. An iterative 2DSA step is performed at the end. Using the final 2DSA model for each wavelength, a time-synchronized finite element model is computed for each wavelength, generating a multi-wavelength surface (see Figures 3, 4). The resulting simulation is decomposed into the basis spectral vectors to generate a new dataset for each spectrally unique component (see Equation 1).⁴

$$C_{MWL} = \underset{\text{NNLS}}{\chi_{\alpha}} \begin{matrix} \text{HSA} \\ \left[\begin{array}{c} \epsilon_{a1} \\ \epsilon_{a2} \\ \dots \\ \epsilon_{ai} \end{array} \right]_{r,t} \end{matrix} + \underset{\text{HSA-PPIX}}{\chi_{\beta}} \begin{matrix} \left[\begin{array}{c} \epsilon_{b1} \\ \epsilon_{b2} \\ \dots \\ \epsilon_{bi} \end{array} \right]_{r,t} \end{matrix}$$

Equation 1. Non-negative least squares of the multi-wavelength dataset by decomposing wavelength profiles into 2 basis vectors representing the intrinsic absorbance spectra of HSA and HSA-PPIX-Sn

This approach will generate a scalar concentration for each radial position and scan time for each spectrally unique component, resulting in separate hydrodynamic experimental data for each spectrally unique species. In this case, we used the absorbance spectra of apo-HSA and HSA-PPIX-Sn to separate the signals into two spectrally distinct hydrodynamic datasets. These datasets were analyzed by Monte Carlo Analysis⁵ with either 2DSA or the parametrically constrained spectrum analysis (PCSA).⁶ A plot of the hydrodynamics as a function of wavelength can reveal spectral properties of each species⁷ as shown in Figure 5.

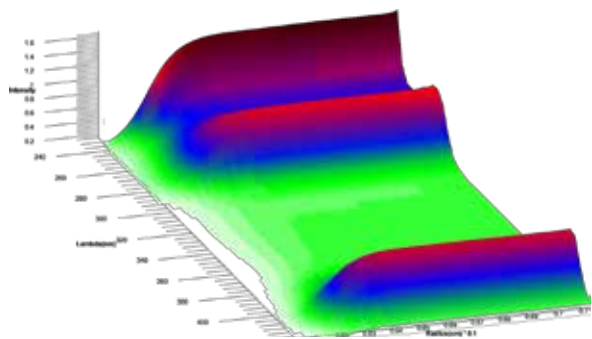


Figure 3. 25th scan of time synchronized finite element model

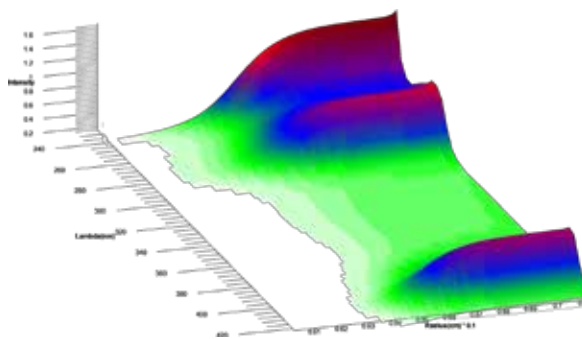


Figure 4. 50th scan of time synchronized finite element model

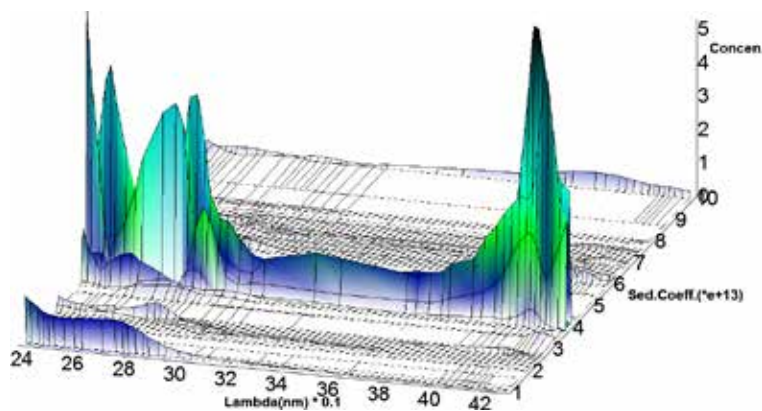


Figure 5. Hydrodynamic properties as a function of wavelength depicting spectral properties

Results

The goal of this study was to identify if purified HSA-PPIX can be reliably distinguished from free HSA by using multiwavelength enabled AUC⁸. To this end, we mixed apo-HSA with the previously prepared HSA-PPIX-Sn complex. The results from the Monte Carlo analysis of the separated hydrodynamic datasets are shown in Figure 6. These results show that separating the signals into two distinct hydrodynamic data sets allow us to determine the concentration and the hydrodynamic parameters for each spectrally unique component in solution. These results also indicate that the sedimentation coefficient of the porphyrin-complexed HSA is slightly higher than the apo-HSA.

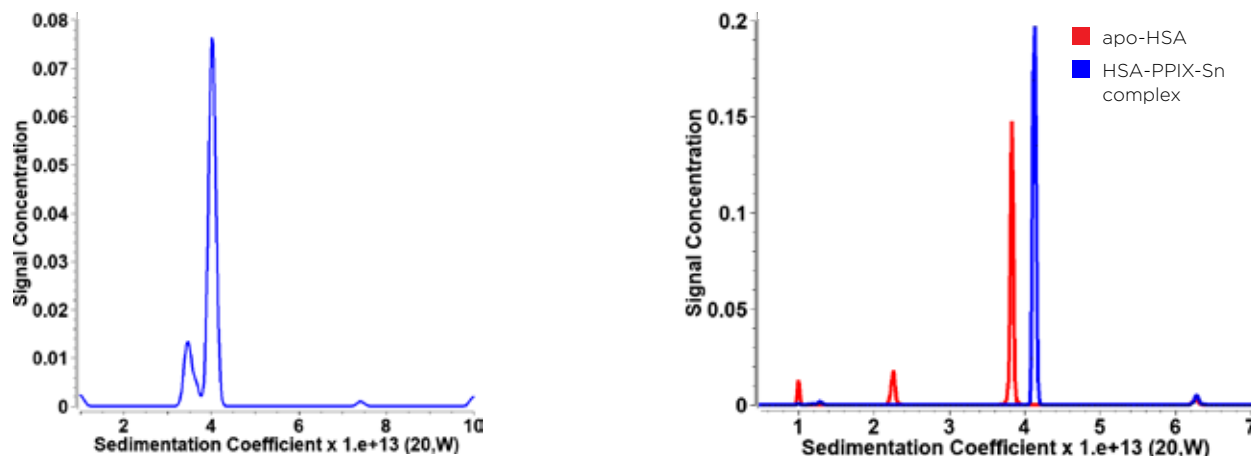


Figure 6. A single wavelength (278 nm) experiment (left) shows two peaks but the species represented by those peaks is unable to be discerned. The multiwavelength experiment (right) allows us to baseline separate each component. This allows us to discern which peak represents apo-HSA (red) and which peak represents the HSA-PPIX-Sn complex (blue).

The difference in absorbance spectra for free HSA and HSA bound to PPIX can be used to separate the hydrodynamic data into data sets that represent each of the two species. As can be seen in Figure 6, the ability to spectrally separate individual species, even if they are hydrodynamically very similar, can be baseline-separated by this method, while a single wavelength (278 nm, which is the peak absorbance for apo-HSA) shows two peaks, though it is unclear which represents the apo HSA and which the HSA-PPIX-Sn species. This results in much higher resolution for any AUC experiment than was possible before. Furthermore, for mixtures containing multiple species with different absorbance spectra, it is now possible to derive intrinsic extinction spectra for each species, if they are hydrodynamically well-separated (see Figures 5 and 6). In this case however, the two species present in this mixture are hydrodynamically very similar and unique spectra are difficult to discern (Figure 5). Clearly, this improvement has far-reaching impact on the future of AUC experiments, especially for the study of interacting systems where the interaction partners have unique spectral properties.

References

1. Hu J, Demeler B, Brancalion L. Experimental and Computational Study of the Binding of Metalloporphyrins to the Metal Binding Sites of Human Serum Albumin (2017) Unpublished
2. Demeler, B Methods for the Design and Analysis of Sedimentation Velocity and Sedimentation Equilibrium Experiments with Proteins. Cur. Protoc. Prot. Sci. (2010) Chapter 7:Unit 7.13.
3. Brookes E, Cao W, Demeler B A two-dimensional spectrum analysis for sedimentation velocity experiments of mixtures with heterogeneity in molecular weight and shape. Eur Biophys J. (2010) 39(3):405-14.
4. Gorbet GE, Pearson JZ, Demeler AK, Cölfen H, and B. Demeler. Next-Generation AUC: Analysis of Multiwavelength Analytical Ultracentrifugation Data Methods in Enzymology, Aug 2015. doi:10.1016/bs.mie.2015.04.013
5. Demeler B and E. Brookes. Monte Carlo analysis of sedimentation experiments. Colloid Polym Sci (2008) 286(2) 129-137
6. Gorbet G., T. Devlin, B. Hernandez Uribe, A. K. Demeler, Z. Lindsey, S. Ganji, S. Breton, L. Weise-Cross, E.M. Lafer, E.H. Brookes, B. Demeler. A parametrically constrained optimization method for fitting sedimentation velocity experiments. Biophys. J. (2014) Vol 106(8), pp1741-1750
7. Karabudak E, Brookes E, Lesnyak V, Gaponik N, Eychmüller A, Walter J, Segets D, Peukert W, Wohlleben W, Demeler B, H Cölfen. Simultaneous Identification of Spectral Properties and Sizes of multiple Particles in Solution with sub-nm Size Resolution. Angewandte Chemie 2016 Sep 19;55(39):11770-4.
8. Zhang J, Pearson JZ, Gorbet GE, Cölfen H, Germann MW, Brinton MA, Demeler B. Spectral and Hydrodynamic Analysis of West Nile Virus RNA-Protein Interactions by Multiwavelength Sedimentation Velocity in the Analytical Ultracentrifuge. Anal Chem. 2017 Jan 3;89(1):862-870.